

Electric field spikes formed by electron beam-plasma interaction in plasma density gradients

H. Gunell and T. Löfgren

*Division of Plasma Physics, Alfvén Laboratory,
Royal Institute of Technology,
SE-100 44 Stockholm, Sweden*

(Dated: Received 14 February 1997; accepted 5 May 1997)

In the electron beam-plasma interaction at an electric double layer the beam density is much higher than in the classical beam-plasma experiments. The wave propagation takes place along the density gradient, that is present at the high potential side of the double layer. Such a case is studied experimentally by injecting the electron beam from a plane cathode, without any grids suppressing the gradient, and by particle simulations. The high frequency field concentrates in a sharp “spike” with a half width of the order of one wavelength. The spike is found to be a standing wave surrounded by regions dominated by propagating waves. It forms at a position where its frequency is close to the local plasma frequency. The spike forms also when the electric field is well below the threshold for modulational instability, and long before a density cavity is formed in the simulations. Particle simulations reveal that, at the spike, there is a backward travelling wave that, when it is strongly damped, accelerates electrons back towards the cathode. In a simulation of a homogeneous plasma without the density gradient no spike is seen, and the wave is purely travelling instead of standing.

I. INTRODUCTION

High frequency plasma waves that are driven by an electron beam-plasma instability can form spatially concentrated “HF spikes”, with a full width at half maximum of about one wavelength. Such a spike has previously been observed at an electric double layer, in a region on the high potential side of the double layer where a density gradient, which is produced by the double layer, exists.¹ The spike was found to have an irregular motion back and forth with a velocity of the order of the ion acoustic velocity. When it passes a stationary probe, low frequency bursts of HF waves are observed on the probe signal. The bursts reported¹ were 1 - 5 μ s long, and the moving HF spike causing them was found to be 10 - 20 mm (about one wavelength) wide. The HF spike was moving in the inhomogeneous plasma on the anode side of the double layer, in an approximately 100 mm wide region, beginning about 50 mm from the double layer. The growth length and the amplitude of these HF spikes were found to agree fairly well with theoretical expectations from linear growth^{2,3} and beam trapping^{2,4}. Approximate values of these quantities are included in Table I. However, the small extent in the beam direction could not be explained, and proposed explanations, as Langmuir collapse, could not be matched to the experimental data. However, the amplitude decrease after the amplitude saturation agreed fairly well with thermal Landau damping, suggesting that the beam is strongly scattered and thermalized by the spike.

Similar HF spikes have been studied in computer simulations and in a different experiment using a hot Lanthanum hexaboride cathode as source of the electron beam⁵. In this paper we have examined three experimental cases, with acceleration voltages ranging from 35 to 210 volts, and the results are compared with com-

puter simulations. No attempt to minimize the density gradient by grids was made, and accordingly the cathode sheath and its presheath gave a density gradient similar to the one at a double layer. Some plasma parameters from the experiments are shown in Table I. In the double layer experiment the electrons were accelerated by the 27 V double layer voltage. The higher voltage in the cathode experiments yields beam energies high enough to excite an electric field strength larger than the threshold for Langmuir collapse⁶, though the spikes are formed also for fields below that threshold. In the experiments, both with the cathode and the double layer, the HF spike appears in a region where a plasma density gradient exists. Similar results are obtained by computer simulations⁵.

The importance of density inhomogeneities for the growth of plasma instabilities was pointed out by Böhmer et al.⁷, who studied a plasma that was irradiated by microwaves. They developed a cold plasma model where the spatial growth rate of the instability was limited by collisions. In our case collisions are negligible, and the spatial growth is limited by thermal effects. The importance of density gradients was also studied by Bollinger et al.⁸, who made experiments showing how plasma waves could concentrate to inhomogeneous plasma regions. In the present work we present detailed measurements of the plasma waves in such gradients.

The experiment is modelled by a one dimensional, electrostatic particle in cell simulation. An electron beam is injected and accelerated in the cathode sheath that develops self-consistently. The beam interacts with the background plasma as it travels into a plasma density gradient. This beam-plasma interaction produces an HF spike as in the experiments. The simulation thus reproduces the experiment and contributes information that is useful in understanding of the physics behind the phenomenon. Two different beam voltages are considered,

TABLE I: Some experimental data of interest for comparison between the different cases. The linear spatial growth rate k_i was calculated for an unstable wave growing on a cold thin beam in a plasma², and though it does not include Landau damping $1/k_i$ gives a fair estimate of the growth length.

	DL - 27 V	Cathode - 35 V	Cathode - 95 V	Cathode - 210 V
n_b/n_0 (approx.)	0.03	0.3	0.25	0.2
$k_B T_e/e$	4.5 V	9 - 11 V	5 - 8 V	15 - 20 V
v_b	$3.1 \cdot 10^6$ m/s	$3.5 \cdot 10^6$ m/s	$5.8 \cdot 10^6$ m/s	$8.6 \cdot 10^6$ m/s
$n/\frac{dn}{dx}$ (at the spike)	120 mm	45 mm	50 mm	75 mm
λ	10 mm	9 mm	14 mm	25 mm
$1/k_i$ (calculated)	5 mm	3 mm	4 mm	6 mm
\hat{E}_{\max}	3.5 kV/m	2.7 kV/m	9.3 kV/m	18 kV/m
\hat{E}_{thr}	6.1 kV/m	10 kV/m	3 kV/m	6 kV/m
B_z	4 mT	7 mT	3 mT	3 mT

and the results are compared with results of the detailed measurements of the HF electric field.

The investigations show that HF spikes develop in all the experimental cases with various acceleration voltages, and in the simulations only when a density gradient is present in the interaction region. The HF spike is a narrow region dominated by a standing wave and is surrounded by regions dominated by travelling waves. The standing wave is a superposition of a forward and a backward travelling wave, both of which are found in different regions of the plasma column. In the simulation with high beam energy, where the oscillating electric field is strong, acceleration of some particles out of the distribution to negative velocities, of the same order as the beam velocity is seen. This is a clear evidence of the existence of a high amplitude wave with negative phase velocity, transferring momentum to resonant particles. The HF spike provides a short interaction-length mechanism for beam scattering, that differs from the classical model for amplitude saturation by trapping of beam electrons in a travelling wave.

II. EXPERIMENTAL SETUP AND PLASMA DIAGNOSTICS

The experimental device was a large cylindrical stainless steel tank (Fig. 1). A ring shaped anode (outside diameter 33 cm, inner diameter 100 mm) is located near the right hand side of the chamber. The plasma is formed by a discharge between this anode and a Lanthanum hexaboride cathode (diameter 35 mm), that is concentric with the anode. A metal plate at floating potential is placed at about 60 cm from the cathode, and a plasma column is formed between the plate and the cathode. The cathode is heated to about 1500 °C. A beam is injected through the plasma by applying a negative voltage to the cathode. Most of the applied voltage is concentrated in a cathode sheath. Three cases with 35, 95, and 210 volts over the sheath respectively is investigated. The electrons must move across the magnetic field lines to reach the anode

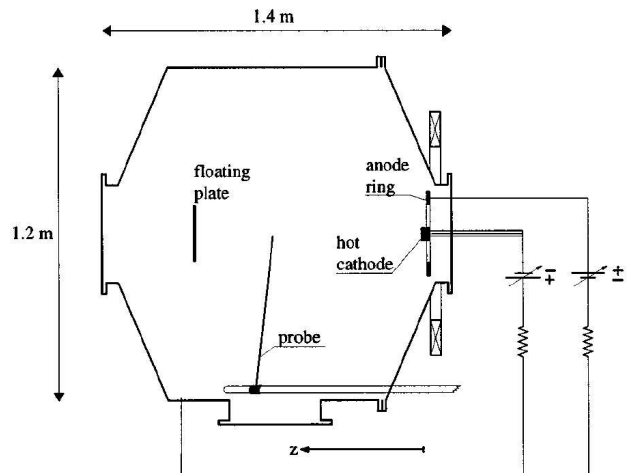


FIG. 1: The Green tank in which the experiments were performed. The electrons are accelerated in the cathode sheath and travels to the left in the figure.

ring. The magnetic field is produced by the coil on the right hand side of the chamber, and has a mirror field topology. However, the magnetic field is approximately constant over region where the beam-plasma interaction occurs and gives an electron gyro radius of about 1 mm there. The background gas was argon at $1 \cdot 10^{-4}$ mbar.

The electric field of the high frequency plasma waves was measured with double probes matched to 50Ω cables.⁹ The probe consists of two parallel 10 mm long wires, that are 0.5 mm apart, and have a diameter of 0.07 mm. The quantity measured is the HF current flowing between the two wires because the low matching resistance means that the wires are effectively short-circuited. In the interpretation of the probe signals, the elsewhere⁹ derived, relation between the electric field and the measured current is used:

$$E_0 = \frac{i}{\omega C (b^2 - 4r^2)^{1/2}} \quad (1)$$

where E_0 is the electric field of the wave, i is the measured current, C is the vacuum capacitance between two parallel cylindrical wires, b is the distance between the wires, and r is the wire radius. To avoid the disturbance from the probe shafts, the last few centimetres of these are substituted with naked wires (diameter 0.07 mm) that are twisted into a spiral.¹ The spiral part of the probe does not pick up any electric field since the charge that is accumulated on one half-turn of the spiral is cancelled by the charge on the neighbouring half-turn.

The measurements of the plasma potential were made using electron emitting probes and the density and temperature were found from analysis of Langmuir probe characteristics. Density measurements in the presence of a strong HF electric field meet some difficulties. Due to the nonlinearity of the probe characteristics the oscillating plasma potential will give a DC-component in the electron current. One would expect to underestimate the electron current to a probe that is biased at the plasma potential. By inserting an inductance close to the probe tip the HF impedance between the probe and ground is increased, and hence the HF current and the HF voltage drop over the sheath surrounding the probe is decreased. The characteristics of two cylindrical Langmuir probes is shown in Fig. 2 (a). The only difference between the probes in Fig. 2 (a) is that one of them has an inductance of $L = 0.21$ mH inserted in the coaxial probe shaft, only 10 cm from the probe tip. It is seen from Fig. 2 that, for the range of probe voltages considered, the probe with the inductance gives a higher measure of the current than the probe without an inductance. Using a circuit model of the probe (Fig. 2 (b)) we can calculate what fraction of the HF voltage that falls over the sheath around the probe. The sheath is modelled by the capacitance C . The resistor R used to measure the current was 1000Ω . The impedance of the sheath is $z_1 = 1/j\omega C$ and the impedance between the probe and ground is $z_2 = R + j\omega L$. Assuming a harmonic oscillation in the plasma potential the fraction of the HF voltage that falls across the probe sheath is

$$\frac{z_1}{z_1 + z_2} = \frac{1}{1 - \omega^2 LC + j\omega RC} \quad (2)$$

The resonance frequency $\omega_{res} = (LC)^{-1/2}$ was found by measurements of frequency spectra of the probe circuit with and without the inductance. The capacitance $C = 0.62$ pF could then be calculated. The absolute value of $z_1/(z_1 + z_2)$ is with these parameters below 0.005 for frequencies above 200 MHz. We hence conclude that the HF oscillations are sufficiently suppressed to be of no significance for the current measurement. At the resonance frequency $\omega_{res}/2\pi \approx 14$ MHz, $|z_1/(z_1 + z_2)| = 1/\omega RC \approx 18$, and there is a risk of an error due to the contribution to the DC current from oscillations at frequencies close to the resonance frequency. However, measurements of frequency spectra, show that the oscillations at frequencies close to ω_{res} give a negligible contribution to the DC probe current.

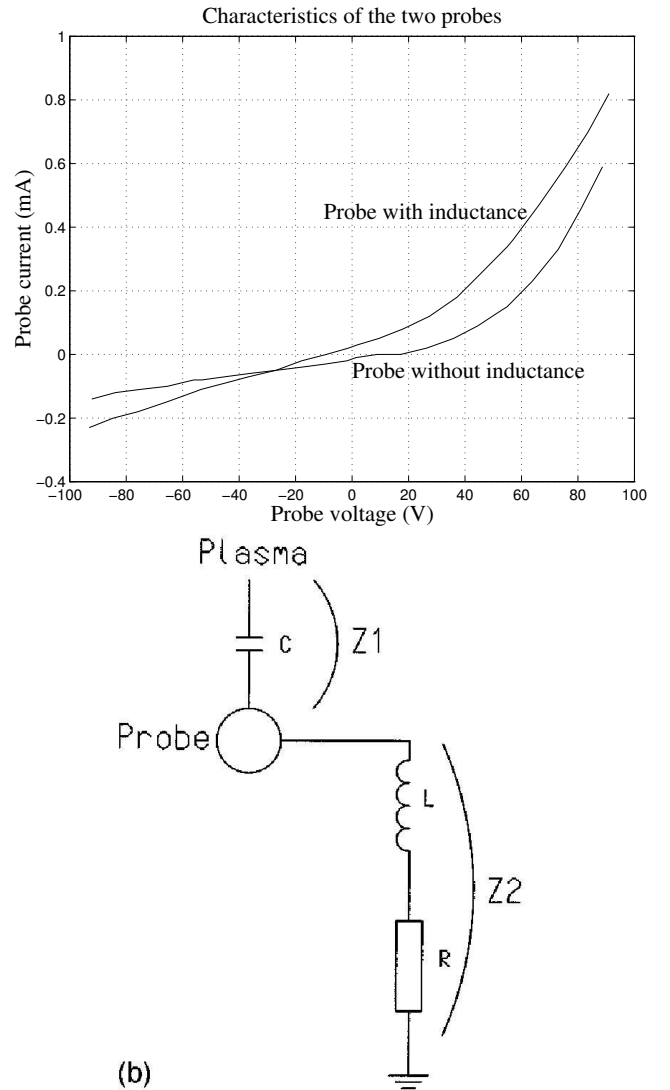


FIG. 2: Characteristics of two Langmuir probes (a). One with and one without an inductance in the probe shaft. The influence of the HF oscillations on the DC current is reduced by the insertion of the inductance. The probe without inductance gives an underestimated measurement of the electron current at plasma potential.

Panel (b) shows a circuit model of the probe with the inductance inserted in the coaxial probe shaft. The capacitance C is used to model the sheath around the probe for these high frequencies. The inserted inductance L was in our case 0.21 mH, and the resistance R used for the measurement of the current was 1000Ω .

III. EXPERIMENTAL RESULTS

A hot, plane cathode with a diameter of 35 mm is used as the beam source. Three different acceleration voltages are used and the density is $1 - 2 \cdot 10^{15} \text{ m}^{-3}$ in all the three cases. Fig. 3 shows the plasma potential, density and the maximum high frequency electric field amplitude during a long time recording by one probe that is moved

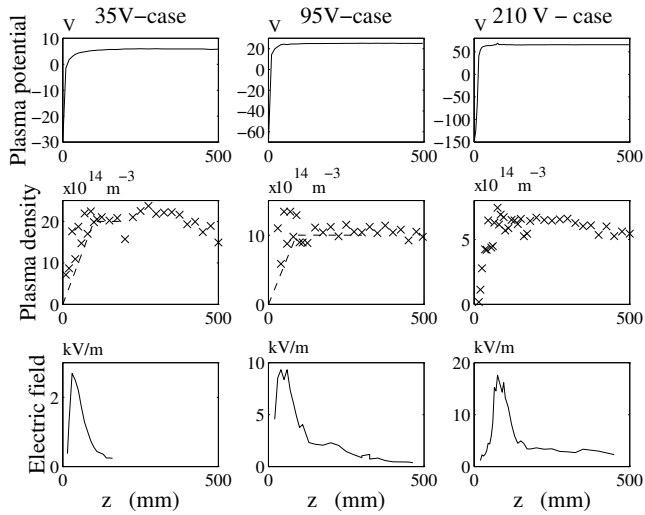


FIG. 3: Plasma potential, plasma density and the maximum electric field strength as functions of the axial coordinate z , for the 35, 95, and 210 V cases. The dashed lines in the experimental density plots of the 35 and 95 V cases show the initial density of the corresponding simulations.

along the axis of the experiment. The coordinate z refers to the distance from the cathode. We define the HF region as the range in z coordinates within which the HF oscillations ever exists, in contrast to the HF spike which is the momentary extent of the HF waves. The widths at half amplitude of the HF regions observed by the probe are approximately 50, 70, and 100 mm in the 35, 95, and 210 V cases respectively.

As observed in the double layer case,¹ the HF spike has an irregular motion back and forth within the HF region with a velocity of the order of the ion acoustic velocity. This irregular motion is probably due to fluctuations on the time scale of the ion motion. The HF spike extends typically 1 cm, about one wavelength, in the beam direction.

The HF field is axially directed over most of the plasma column cross-section which is determined by the diameter of the cathode. At the radial boundaries, the magnitude of the electric field drops to very small levels, in the plasma outside the beam region.

To measure the HF electric field of the wave in space and time a conditional sampling technique was used to pick out relevant subsets of data from the signals recorded in the turbulent plasma, by three probes A, B, and C. Probe A is closest to the cathode, probe B is in the middle, and probe C is further out. Probe B was placed in the position where the highest wave field amplitudes could be observed. The two other probes were then moved to various distances from probe B and the signals from the three probes were simultaneously recorded by the oscilloscope. Similar events from the data were selected using a conditional sampling method. The triggering condition used was that a peak, within a certain specified range of electric field strengths, must be present at probe B at

the triggering time and that the amplitude, measured by probe B, must be constant within $\pm 1\%$ over at least two wave periods. In cases where there were several “hits” for the same probe distance the average field from these was used.

Grey-scale plots of the electric field strength as a function of space and time are shown in Fig. 4, for comparison between the three cases. It is seen that there is a region of standing waves around the point in space where the electric field has its maximum, and that the field maximum is surrounded by regions dominated by travelling waves. In Fig. 5 the maximum electric field during ± 5 ns from the triggering time, the same time interval as the Fig. 4, is shown as a function of z . This gives a picture of the instantaneous shape of the HF spike. The HF region according to the lower panels of Fig. 3 is shown for comparison (solid curves). The width of the moving spike is much smaller than the width of the HF region. The existence of a narrow HF spike has also been observed in double layer (DL) experiments¹. Such a spike is clearly present in the 35 V case. In all three cases there is a region dominated by a standing wave. In the 35 V and 95 V cases it is around $z = 45$ mm, and in the 210 V case its centre is at about $z = 65$ mm. Outside this region a forward (in the direction of the beam) travelling wave is dominating. Its phase velocity is slightly below the beam velocity as expected for a beam-driven plasma oscillation. Though the forward travelling wave is dominating here, amplitude modulations can be seen, indicating the interference with a backwards travelling that has a lower amplitude. A line with a slope corresponding to the phase velocity of such a backwards travelling wave should trace the amplitude maxima created by the constructive interference between the two waves. The slope of such a line shows that the backward travelling wave has a phase velocity about equal to that of the forward wave. The region where the HF spike is observed is located where there is a gradient in the plasma density.

An HF spike in a density gradient was also found in an experiment where the beam was generated by acceleration of electrons in an electric double layer.¹ The similarity of the waves in the two discharges were found in spite of the very different experimental conditions. In the DL case the electron beam was going into the weak magnetic mirror field, whereas in the case here it goes out of it. The beam emitted from the cathode is much colder than the beam of the DL case. The relative beam density $\eta = n_b/n_0$ was 3% in the DL case, and 20 - 30% in the cathode case. The main similarity was the voltage by which the beam electrons were accelerated. It was 35 V in the simulation and the cathode experiment, which is not too far from the 27 V double layer voltage.

The main features are the same in the higher voltage cases as in the 35 V case. However the beam and phase velocities are higher, the wavelength longer, and the whole structure is wider. The amplitude is non-monotonous making it difficult to pick out a single HF spike. The electric field is stronger in the 95 and 210

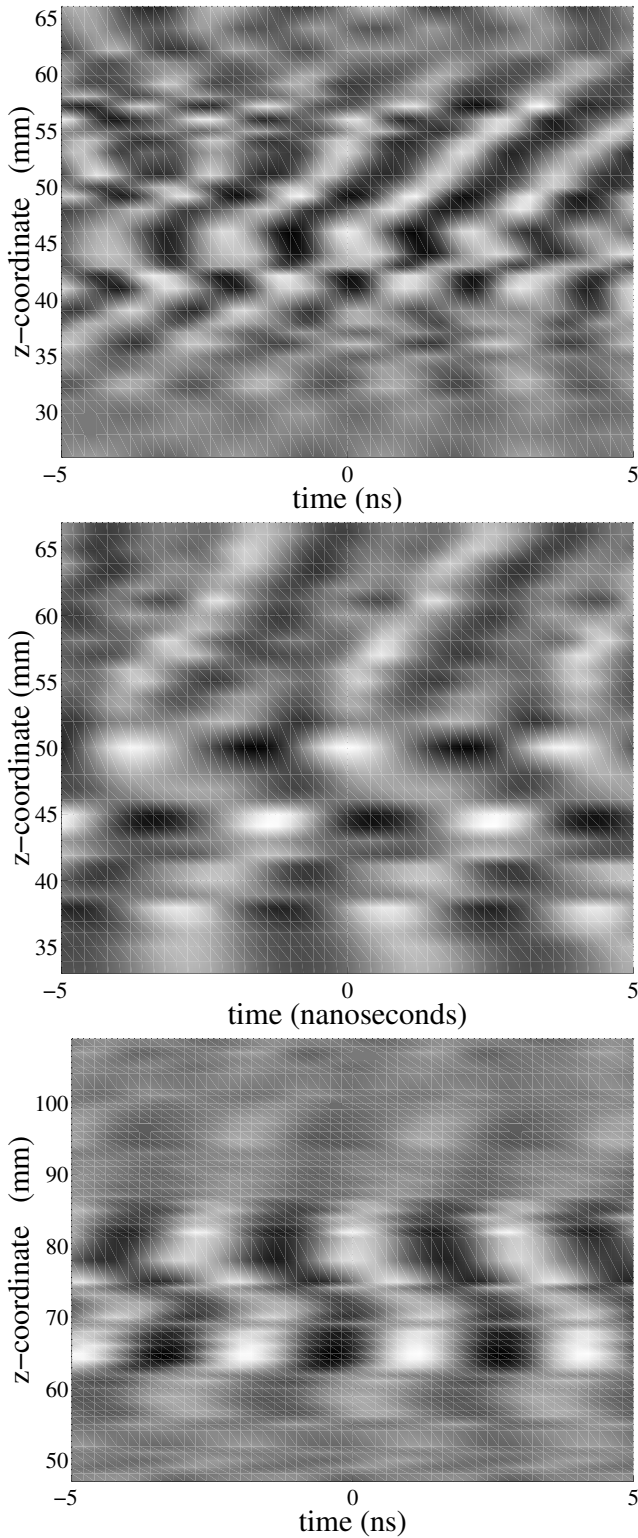


FIG. 4: The electric field strength in the three cases as a function of time and space displayed as grey-scale plots. The 35 V case is shown in (a), the 95 V case in (b), and the 210 V case in (c). The triggering condition was that a peak in the E -field at the triggering point had to be between 1.0 and 1.5 kV/m in the 35 V case, between 5.0 and 5.5 kV/m in the 95 V case, and between 8.0 and 10 kV/m in the 210 V case. The condition that the amplitude had to be within $\pm 1\%$ for at least two wave periods was also applied.

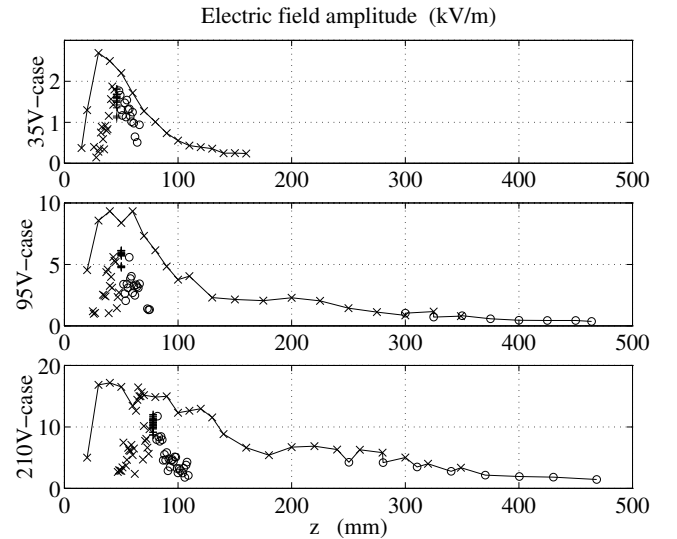


FIG. 5: The maximum electric field as a function of z measured within the same short time interval as is shown in Fig. 4. Measurements made with probe A, which is closest to the cathode, are marked “x”, probe B “+”, and probe C “o”. There is clearly an HF-spike, as in the double layer case. The solid curves show the maximum electric field that could be observed as a function of z .

V cases, and as is seen from Table I over the threshold field for Langmuir collapse, \hat{E}_{thr} .⁶ That the electric field is above that level is a necessary but not sufficient condition for collapse, and we do not see any signs of collapse, in our weakly magnetised plasma. Even if no collapse occurs the electric field is strong enough to influence the plasma density through the ponderomotive force, as is seen by the computer simulations described in the following section. No density cavity could be detected experimentally. However, due to the presence of fluctuations and the motion of the spike, any cavities caused under influence of the ponderomotive force is expected to be long and shallow, and hence not detectable by our density probe.

IV. COMPUTER SIMULATIONS

The simulations were performed using the particle-in-cell code, PDP1.¹⁰ The plasma parameters used in the simulations were chosen as close to the experimental parameters, shown in Table I, as possible. The 35 and 95 V cases were simulated using 200 and 300 mm long plasma diodes respectively. The background electron temperature was 5 eV. The initial density increased linearly from zero at the left hand boundary ($z = 0$) to a constant value ($2 \cdot 10^{15} \text{ m}^{-3}$ in the 35 V case and $1 \cdot 10^{15} \text{ m}^{-3}$ in the 95 V case) in the right hand part of the plasma. For reference, this profile is shown as dashed curves in the experimental density plots of Fig. 3. The time-step Δt used in the simulation was $1.25 \cdot 10^{-11}$ s, and the length-

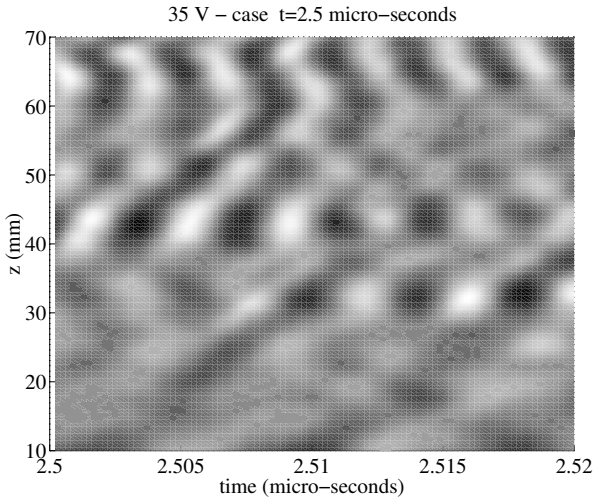


FIG. 6: The electric field strength in the simulation of the 35 V case as a function of time and space displayed in a grey-scale plot. The time t is between 2.50 and 2.515 μs

step Δz was 0.5 mm. This gives $\omega_{pe} \cdot \Delta t / 2\pi \leq 0.005$, and $\Delta z \leq \lambda_D$.

A half-Maxwellian distribution of electrons, with a temperature of 0.15 eV for the full Maxwellian distribution, was injected at $z = 0$ and accelerated in a cathode sheath that developed self-consistently. These electrons formed the beam. Since the plasma is at positive potential the left ($z = 0$) electrode was biased to -20 and -55 V respectively to achieve the 35 and 95 V beam energies. The resulting time averaged potential as a function of z then became similar to the experimentally obtained potential curves shown in Fig. 3.

As in the experiment a beam-driven HF region appeared in the simulation. The electric field in the 35 V simulation, as a function of time and space, is shown in Fig. 6 as a grey-scale plot. The electric field was recorded between $t = 2.5 \mu\text{s}$ and $t = 2.515 \mu\text{s}$. The simulated electric field should be compared to the field data obtained from the measurements which are described in section III. There is a conspicuous similarity between Fig. 6 and Fig. 4(a), which shows the measured electric field in the 35 V experimental case. In both cases there is a narrow region with standing waves at $z \approx 40$ mm. Outside the HF spike a forward travelling wave dominates over the backwards travelling one.

A small depletion of the plasma density can be seen in the simulation of the 35 V case at the same place as the peak in the electric field after a sufficiently long time. This indicates that the plasma is pushed away by the ponderomotive force associated with the narrow electric field peak. However, the field spike is seen before the density depletion appears, and when the simulation is run for several microseconds, the peak does not change size or move, significantly. Hence we conclude that the density depletion has little or no influence on the wave itself in this case. An example of the density depletion is

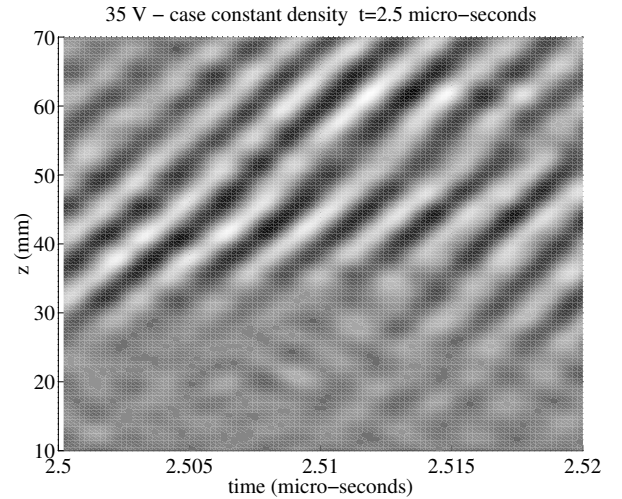


FIG. 7: The electric field strength at time t between 2.50 and 2.515 μs in a simulation where the density is constant, and equal to $2 \cdot 10^{15} \text{ m}^{-3}$ throughout the simulated system. The other parameters are the same as in the simulation shown in Fig. 6. When the density is constant no HF spike is seen. The dominating wave is forward travelling.

given in the 95 V case shown below.

The significance of a density gradient for the formation of the HF spike has been investigated by running the simulation with a constant plasma density of $2 \cdot 10^{15} \text{ m}^{-3}$. The other parameters were kept the same as in the previous runs. No spike appears even when the simulation is allowed to run for several microseconds. For comparison, it appeared before 1.0 μs in the simulation with a gradient. The waves to the right of $z = 40$ mm where they had grown to full amplitude, were purely forward travelling, and were present at large amplitude in the whole plasma. The amplitude was 3 - 4 kV/m in both the simulation with and that without gradient. Fig. 7 shows an z, t -diagram of the electric field in the simulation with a constant plasma density. This should be compared with Fig. 6, which shows the same thing for the simulation with a density gradient. As noted in section III the experimentally detected HF spikes were always found in density gradients, both in the experiments with a cathode and in the double layer experiments.

Two sets of electric field data from a simulation that is run with 95 V cathode sheath voltage is shown in Fig. 8, for times $2\mu\text{s}$ and $3\mu\text{s}$. The electric field is stronger in the 95 V case where the beam energy is higher which increases the ponderomotive force. Fig. 9 shows the density in the 95 V case at $t = 2\mu\text{s}$ and $t = 3\mu\text{s}$. A cavity is clearly seen after $3\mu\text{s}$, whereas in the 35 V case only a small depletion can be seen. It is also seen that the shape of the spike changes with time much more rapidly in the 95 V than in the 35 V case where the wave structure could be considered as stationary on the micro-second time scale. In both cases the HF spike is seen before the density depletion appears, thus showing that the HF

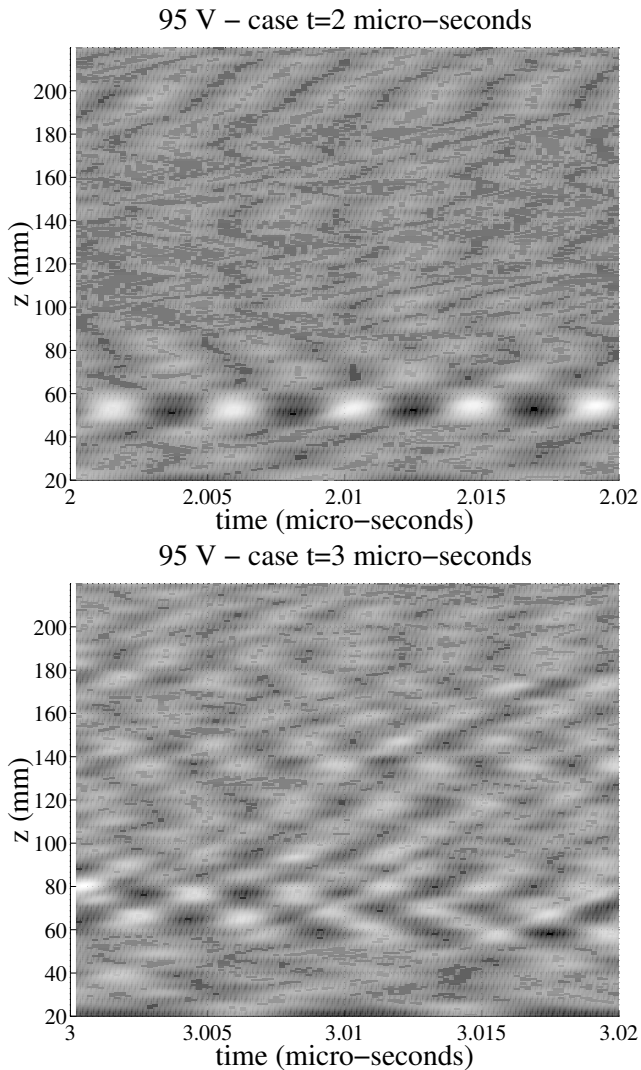


FIG. 8: The electric field strength in the simulation of the 95 V case as a function of time and space. The situation after $2 \mu\text{s}$ is shown in (a), and the electric field after $3 \mu\text{s}$ is shown in (b).

spike is not a result of trapping of radiation.

Fig. 10 shows the electric field in the simulation of the 95 volt case for different times t between $t = 2.0060 \mu\text{s}$ and $t = 2.0080 \mu\text{s}$, with $\delta t = 0.4 \text{ ns}$ between the curves. The curves show how the electric field of the HF spike changes during half a wave period. The electric field in the positive z -direction is at its maximum value at $t = 2.0060 \mu\text{s}$. The dominating amplitude of the HF spike is more evident than in the grey scale plot of Fig. 8. Phase space diagrams show that the beam is destroyed completely during its passage through the HF spike. An example of this is shown in Fig. 11 (a), which shows the phase space of the 95 volt case at $t = 2.0072 \mu\text{s}$. The beam is rapidly dissolved, the hot tail is lost at the anode (not shown), and the warm electrons are mixed with the plasma electrons. The HF spike accordingly provides

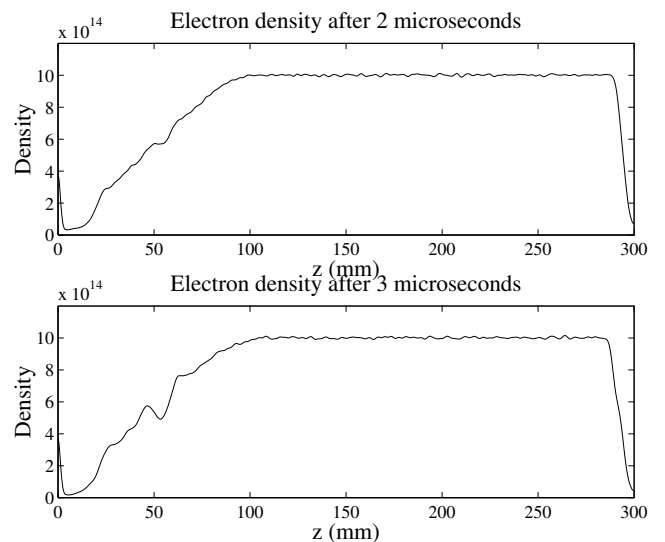


FIG. 9: The plasma density after 2 and $3 \mu\text{s}$ respectively. A density dip is observed at the position of the spike.

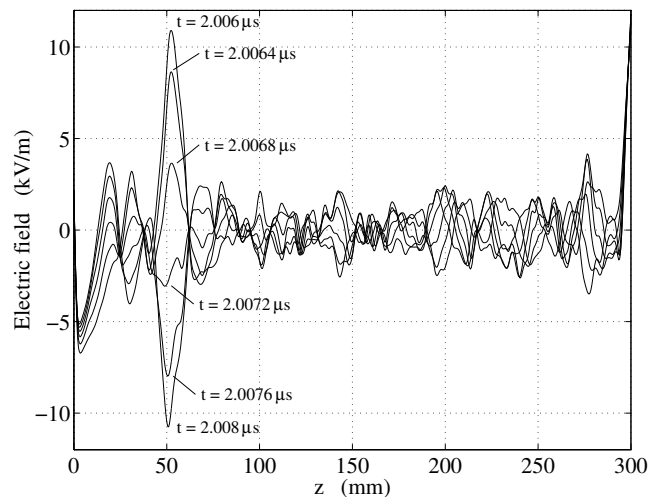


FIG. 10: The electric field in the simulation of the 95 volt case for different times t between $t = 2.0060 \mu\text{s}$ and $t = 2.0080 \mu\text{s}$, with $\delta t = 0.4 \text{ ns}$ between the curves. Half a period of the oscillation is shown. The dominating amplitude of the HF spike is more evident than in the grey scale plot of Fig. 8.

a short interaction-length mechanism for spreading of the electron beam. The acceleration of some particles out of the distribution to negative velocities, of the same order as the beam velocity, is a clear evidence of a high amplitude wave with negative phase velocity. The velocity distribution functions $f(z, v)$ for some z , $0 < z < 120 \text{ mm}$, is shown in Fig. 11 (b) for $t = 2.0072 \mu\text{s}$. A rescaled function, $10f$, is shown as a dotted line, to enhance the tail. The beam component decreases rapidly by the continuity equation and the background plasma increases in density. The flat, thick, tail in the distribution for higher z , does not support growing wave modes.

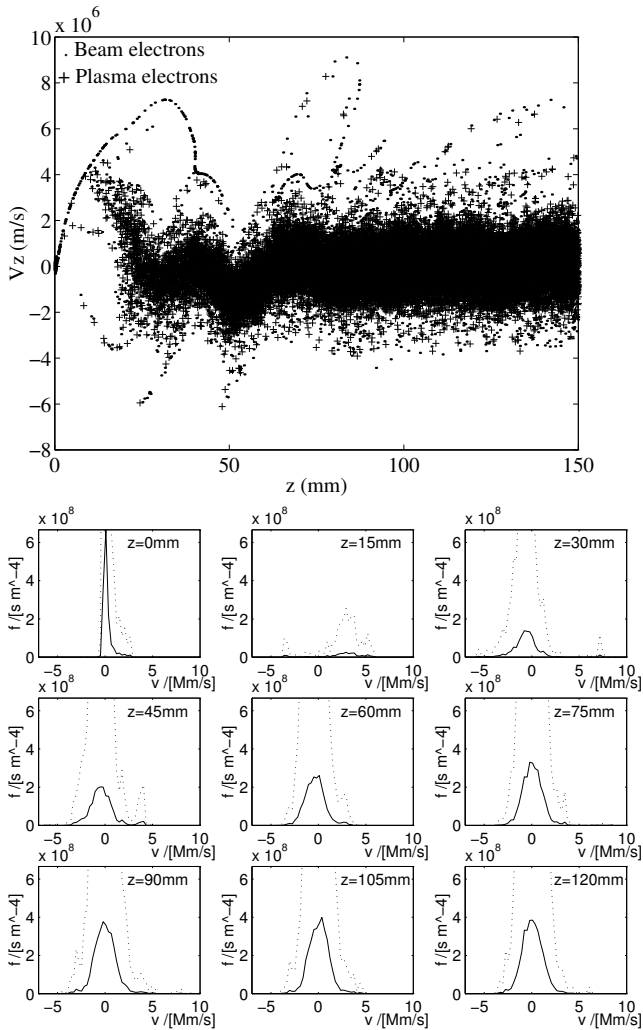


FIG. 11: (a) A phase space diagram of the simulated 95 V case at $t = 2.0072 \mu\text{s}$. The beam is spread completely after passing the HF spike, at $z \approx 45\text{mm}$. To the left of the spike three structures of accelerated particles with negative velocity are evident.

(b) The velocity distribution functions $f(z, v)$ for some z near or at the density gradient. The particles in (a) are distributed linearly to the four neighbouring meshpoints, in a 61 by 61 mesh, including the boundaries. A rescaled function, $10f$, is shown as a dotted line, to enhance the tail. The high spike at the cathode ($z = 0$) is formed by the virtual cathode. This beam component decreases and is shifted by the acceleration in the potential gradient. At the HF spike ($z \approx 45\text{mm}$), the beam is spread and a flat tail is formed.

V. CONCLUSIONS

The measurements show that there is a narrow HF spike when the voltage drop over the cathode sheath is 35 volts. In all investigated cases, with voltages 35, 95, and 210 V, there is a region dominated by a standing wave surrounded by regions dominated by travelling waves and the HF spike forms in a region with a density gradient.

Results similar to the experimental results are obtained in the computer simulations. The appearance of the HF spike in the different experiments (double layer and cathode) and in the simulations shows that the HF spike is a general phenomenon occurring when electron beams travel along plasma density gradients. It is shown by the simulations that the stationary HF spikes offer a short interaction-length for beam scattering, differing from the classical model for amplitude saturation by trapping of beam electrons in a travelling wave. The strong electric field of the spike can accelerate electrons in the direction of the cathode with a velocity of the same order as the beam velocity, showing the presence of a high amplitude wave that has a phase velocity in the direction opposite to the beam.

VI. DISCUSSION

The HF spike is a standing wave, and the presence of a density gradient is important for its formation. What still remains to be explained is its width and position. We here propose two physical mechanisms that may cause the observed phenomenon. The explanation could be either of those, but it is also possible that both are at work at the same time.

First there is the possibility of wave-wave interaction¹¹. The beam wave would grow to a high amplitude and then split up into a backwards travelling Langmuir wave and a forward travelling ion wave, through a parametric process. The standing wave that is observed would then be a superposition of, the backward travelling and the original, electron waves. Fluctuations on the ion time scale have been observed in a previous experiment¹. Those observations and the changes between $t = 2\mu\text{s}$ and $t = 3\mu\text{s}$ would then indicate a modulation by ion waves. It is, however, questionable if this kind of interaction will occur in a highly inhomogeneous plasma. A backward wave formed by wave-wave interaction would propagate at a different phase velocity, which is less favourable for the constructive interference that is observed as a standing wave pattern.

The other possibility is that the wave cannot propagate into the region of higher density ($z > z_{\text{spike}}$). A Langmuir wave would not propagate in regions where the plasma frequency exceeds the wave frequency, and no beam mode exist after the beam spread. A Langmuir wave in a gradient, or boundary layer, will be reflected. The reflected wave then adds to the incoming unstable wave yielding a high amplitude standing wave.

In both cases the, backward travelling, electron wave must be strongly damped, or else the width of the HF spike would be much greater than observed. When the backward travelling wave travels into a region with lower density its phase velocity decreases. When the phase velocity reaches a level where there are resonant particles Landau damping starts. The backward wave, with a frequency about $\omega_{p,\text{spike}}$, will propagate as long as the local

plasma frequency ω_p follows, $\omega_p \gtrsim \frac{1}{2}\omega_{p,\text{spike}}$. When the density is even lower, the wave will be strongly Landau damped. For a spike at $z_{\text{spike}} \approx 50$ mm this would happen at $z \approx 35$ mm. This estimate of the extension of the spike is consistent with the presented results. Higher accelerating voltage gives a spike further out on the density gradient, and consequently a broader z -extension of the allowed plasma frequencies. Since higher beam velocities give longer wavelength, the extension could also be an effect of scaling. The damping ejects resonant particles from the distribution function as seen in Fig. 11 (a)

While the reflection mechanism is a first order process, and thus independent of amplitude, wave-wave interactions are of higher order and require large amplitude. Wave-wave interaction could also take place without the presence of a density gradient. If wave-wave interaction was the only cause of the formation of the spike, signifi-

cantly smaller amplitudes would be expected in the simulation without a density gradient, since no HF spike was seen. However, as it is noted in section IV the amplitudes in the two cases are about equal but the spike is absent in the homogeneous case. The reflection mechanism, for the formation of an HF spike, is consistent with the observations, but wave-wave interaction or other processes can also contribute.

Acknowledgments

This work was supported by the Swedish Natural Science Research Council. We wish to thank professor S. Torvén and Dr N. Brenning for valuable discussions.

-
- ¹ H. Gunell, N. Brenning, and S. Torvén, *J. Phys D: Appl. Phys.* **29**, 643 (1996)
² P. Y. Cheung and A. Y. Wong, *Phys. Fluids* **28**, 1538 (1985)
³ T. M. O'Neil and J. H. Malmberg, *Phys. Fluids* **11**, 1754 (1968)
⁴ S. Kainer, J. Dawson, R. Shanny, and T. Coffey, *Phys. Fluids* **15**, 493 (1972)
⁵ H. Gunell, J. P. Verboncoeur, N. Brenning, and S. Torvén, *Phys. Rev. Lett.* **77**, 5059 (1996)
⁶ D. R. Nicholson and M. V. Goldman, *Phys. Fluids* **21**, 1766 (1978)

- ⁷ H. Böhmer, E. A. Jackson, and M. Raether, *Phys. Fluids*. **16**, 1064 (1973)
⁸ L. D. Bollinger, W. Carr, H. Liu, and M. Seidl, *Phys. Fluids*. **17**, 2142 (1974)
⁹ S. Torvén, H. Gunell and N. Brenning, *J. Phys. D: Appl. Phys.* **28**, 595 (1995)
¹⁰ J. P. Verboncoeur, M. V. Alves, V. Vahedi and C. K. Birdsall, *J. Comp. Phys.* **104**, 321 (1993).
¹¹ B. H. Quon, A. Y. Wong, and B. H. Ripin, *Phys. Rev. Lett.* **32**, 406 (1974)